Perturbative analysis of the coherent state transformation in *ab initio* cavity quantum electrodynamics

Peyton Roden and Jonathan J. Foley IV[a)]
Department of Chemistry, University of North Carolina Charlotte, 9201 University City Bldv, Charlotte, North Carolina 07470A

Experimental demonstrations of modified chemical structure and reactivity under strong light-matter coupling have spurred theoretical and computational efforts to uncover underlying mechanisms. Ab initio cavity quantum electrodynamics (QED) combines quantum chemistry with cavity QED to investigate these phenomena in detail. Unitary transformations of ab initio cavity QED Hamiltonians have been used to make them more computationally tractable. We analyze one such transformation, the coherent state transformation, using perturbation theory. Applying perturbation theory up to third order for ground state energies and potential energy surfaces under electronic strong coupling, we show that the coherent state transformation yields better agreement with exact ground state energies. Additionally, we apply perturbation theory up to second order for cavity mode states under bilinear coupling, elucidating how the coherent state transformation accelerates the convergence of the photonic subspace towards the complete basis limit and renders molecular ion energies origin invariant. These findings contribute valuable insights into computational advantages of the coherent state transformation in the context of ab initio cavity quantum electrodynamics methods.

I. INTRODUCTION

Strong interactions between photons resonant with molecular transitions can lead to the emergence of new hybrid light-matter states, known as polariton states, which can effect dramatic changes in chemical structure and reactivity.[1–20] The emerging field of polariton chemistry seeks to understand and leverage these changes in chemical structure and dynamics to perform novel chemistry, and computational modeling has played a key role in shaping this understanding. For one or a few molecules under electronic strong coupling, cavity quantum electrodynamics provides the tools to treat the photonic degrees of freedom and *ab initio* quantum chemistry provides the tools to treat the electronic degrees of freedom. The marriage of these approaches is often referred to as *ab initio* cavity quantum electrodynamics (ai-QED), which has seen a surge of developments in recent years.[18,21–51] Traditional quantum chemistry already presents a challenging example of the many-body problem, and strong coupling to photons introduces additional difficulties that must be overcome to yield accurate and computationally facile approaches.

Unitary transformations have a long history in the development of many-body theories, where a common strategy is to identify or design transformations that bring a many-body Hamiltonian into a representation which is more computationally tractable.[52–56] Recent efforts to develop computationally tractable and predictive methods for molecules under strong light-matter coupling has brought these techniques to bear on ai-QED Hamiltonians to partially decouple the light-matter interactions that arise in this context.[43,57–60] In the Pauli-Fierz Hamiltonian that is the basis for much of the work on ai-QED, there are several examples of unitary transformations that are based upon products of the photonic momentum operator and the matter dipole operator (which is the matter position operator scaled by the electron charge). These transformations impart shifts in the photonic positions and the matter momenta, and render the Pauli-Fierz Hamiltonian diagonal in the infinite coupling limit. In particular, Koch and co-workers[59], as well as Li and Zhang[60], have used such unitary transformations to parameterize reference states for QED Hartree-Fock procedures that have many attractive properties at arbitrary coupling strengths, including energies and orbitals that are fully origin invariant. Reichman and co-workers[43] recently investigated an analogous approach for correlated theories where, similar to the approach of Zhang and Li for QED Hartree-Fock, the transformation is variationally optimized, yielding the so-called Lang-Firsov transformation. In the current work, we focus on a related but simpler unitary transformation known as the coherent state transformation, which shares a similar form as the transformations discussed in the independent investigations in Refs. 43, 59, and 60 with a key difference being it is formulated as a product of the photonic momentum operator with the *expectation value* of the matter dipole operator. The coherent state transformation thus shifts the photonic coordinates but does not transform the matter degrees of freedom. The coherent state transformation has been used to parameterize QED Hartree-Fock reference wavefunctions[29,36] and in correlated ai-QED calculations,[37,41,48,61] and has been shown to yield origin invariant energies (not orbitals), and can significantly accelerate the convergence of the photonic subspace. In this work, we utilize perturbation theory to elucidate how the coherent state transformation engenders these favorable properties in ai-QED calculations. We find that applying the coherent state transformation yields second and third-order estimates to the ground state energy that are in consistently better agreement with exact ground

---

[a)] Electronic mail: jfoley19@charlotte.edu

state across a range of coupling strengths as compared to the same orders without transformation of the Hamiltonian. Furthermore, when we treat the bilinear coupling between matter and photon degrees of freedom as a perturbation to the cavity Hamiltonian, we find that the coherent state transformation decouples the systems to within a magnitude that is related to the error in the reference estimate of the dipole moment expectation value that parameterizes the transformation for a target coupled state. Importantly, this error is manifestly origin invariant, and so this result sheds light on why the coherent state transformation accelerates photon convergence and restores origin invariance in ai-QED calculations.

II. COHERENT STATE TRANSFORMED PAULI-FIERZ HAMILTONIAN

The starting point for many ai-CQED treatments of molecular polariton systems is the Pauli-Fierz Hamiltonian in the dipole approximation[62], which we write in atomic units as

$$\hat{H}_{\rm PF} = \hat{H}_e + \omega\left(\hat{b}^\dagger\hat{b} + \frac{1}{2}\right) - \sqrt{\frac{\omega}{2}}\hat{d}(\hat{b}^\dagger + \hat{b}) + \frac{1}{2}\hat{d}^2. \quad (1)$$

In Eq. 1, $\hat{H}_e$ is the standard electronic Hamiltonian within the Born-Oppenheimer approximation[63], $\hat{H}_{\rm cav} = \omega\left(\hat{b}^\dagger\hat{b} + \frac{1}{2}\right)$ is the bare Hamiltonian for the cavity photon mode where ω represents the frequency and $\hat{b}^\dagger$ and $\hat{b}$ are raising and lowering operators for the photon mode. The last two terms capture the coupling between the photonic and matter degrees of freedom, and are called the bilinear coupling, $\hat{H}_{\rm blc} = -\sqrt{\frac{\omega}{2}}\,\hat{d}\,(\hat{b}^\dagger + \hat{b})$, and dipole self-energy terms $\hat{H}_{\rm dse} = \frac{1}{2}\hat{d}^2$, respectively. In these interaction terms, $\hat{d} = \boldsymbol{\lambda}\cdot\hat{\boldsymbol{\mu}}$ couples the field associated with the photon mode to the molecular dipole operator[64]. The second term $\hat{H}_{\rm cav}$ represents the Hamiltonian for the bare cavity mode, which is a harmonic oscillator with fundamental frequency ω. We may also write this in terms of the canonical position and momentum operators for the cavity photon[65]:

$$\hat{H}_{\rm cav} = \frac{1}{2}\hat{p}^2 + \frac{1}{2}\omega^2\hat{q}^2, \quad (2)$$

where (in atomic units),

$$\hat{p} = i\sqrt{\frac{\omega}{2}}\left(\hat{b}^\dagger - \hat{b}\right) \quad (3)$$

$$\hat{q} = \sqrt{\frac{1}{2\omega}}\left(\hat{b}^\dagger + \hat{b}\right). \quad (4)$$

Next we apply the coherent state transformation to Eq. 1, which has been done, e.g., in QED-Hartree–Fock, QED-CC, QED-CIS, and QED-CASCI[28,29,36,41], yielding the Pauli-Fierz Hamiltonian in the coherent state basis:

$$\hat{H}_{\rm CS} = \hat{H}_e + \hat{H}_{\rm cav} - \sqrt{\frac{\omega}{2}}[\hat{d} - \langle\hat{d}\rangle](\hat{b}^\dagger + \hat{b}) + \frac{1}{2}[\hat{d} - \langle\hat{d}\rangle_0]^2. \quad (5)$$

This follows from a unitary transformation of the Pauli-Fierz Hamiltonian,

$$\hat{H}_{\rm CS} = \hat{U}_{\rm CS}\hat{H}_{\rm PF}\hat{U}^\dagger_{\rm CS}, \quad (6)$$

where the Unitary coherent state transformation is defined as

$$\hat{U}_{\rm CS} = \exp\left(z(\hat{b}^\dagger - \hat{b})\right). \quad (7)$$

where the parameter z may be computed as

$$z = -\frac{\langle\hat{d}\rangle_0}{\sqrt{2\omega}}. \quad (8)$$

The expectation value $\langle\hat{d}\rangle_0$ will depend on the choice of electronic state. Often, the Hartree-Fock (or QED-HF) reference state is used to compute this expectation value, but there are other valid choices.

In this work, we will endeavor to elucidate the properties of the coherent state transformation that can accelerate the convergence of ai-CQED approaches by specifically examining the behavior of the Eqs. 1 and 5 projected onto a subspace of many-electron states that arise from full configuration interaction (FCI) calculations, which is also called a parameterized QED approach (pQED).[18,40,44] In our analysis of these projected Hamiltonians, we will take $\langle\hat{d}\rangle_0$ from the ground state wavefunction from a FCI calculation of the molecule without coupling to the cavity.

1. Perturbation Theory for the Coupled Ground State

We will perform Perturbation theory on the Pauli-Fierz Hamiltonian and on the coherent state Hamiltonian, Eq. 1 or 5 projected onto a truncated basis of adiabatic electronic states. For a discussion of the details of this projection and its use in ai-QED methods, see References 18, 40, 44, and 61 for additional details. The projected molecular electronic Hamiltonian has the form (for both the Pauli-Fierz and coherent-state Hamiltonians):

$$\mathcal{H}_{\rm e} = \sum_\alpha E_\alpha|\psi_\alpha\rangle\langle\psi_\alpha| \quad (9)$$

where E_α and $|\psi_\alpha\rangle$ are the energy eigenvalues of the adiabatic eigenstates, respectively. In this work we will obtain these energies and eigenstates from FCI calculations outside of the cavity, and we will denote the projected Hamiltonian operators with calligraphic font as in Eq. 9. The bilinear coupling terms has the form

$$\mathcal{H}_{\rm PF,blc} = -\sqrt{\frac{\omega}{2}}\sum_{\alpha\beta} d_{\alpha\beta}|\psi_\alpha\rangle\langle\psi_\beta|\left(\hat{b}^\dagger + \hat{b}\right) \quad (10)$$

for the Pauli-Fierz Hamiltonian, and upon coherent state transformation, takes the form

$$\mathcal{H}_{\text{CS,blc}} = -\sqrt{\frac{\omega}{2}}\left(\hat{b}^{\dagger} + \hat{b}\right) \times \left(\sum_{\alpha\beta} d_{\alpha\beta}|\psi_\alpha\rangle\langle\psi_\beta| - \langle\hat{d}\rangle_0 \sum_{\alpha} |\psi_\alpha\rangle\langle\psi_\alpha|\right) \tag{11}$$

where $d_{\alpha\beta} = \langle\psi_\alpha|\hat{d}|\psi_\beta\rangle$ results from dotting the coupling vector into the transition dipole moment between adiabatic states α and β or the total dipole moment of state α when $\alpha = \beta$. Finally, the dipole self energy has the form

$$\mathcal{H}_{\text{PF,dse}} = \frac{1}{2}\sum_{\alpha\beta\gamma} d_{\alpha\gamma} d_{\gamma\beta}|\psi_\alpha\rangle\langle\psi_\beta| \tag{12}$$

for the Pauli-Fierz Hamiltonian and

$$\mathcal{H}_{\text{CS,dse}} = \frac{1}{2}\left[\sum_{\alpha\beta} d_{\alpha\beta}|\psi_\alpha\rangle\langle\psi_\beta| - \langle\hat{d}\rangle_0 \sum_{\alpha} |\psi_\alpha\rangle\langle\psi_\alpha|\right]^2 \tag{13}$$

for the coherent state Hamiltonian.

If we identify our zeroth-order Hamiltonian as

$$\mathcal{H}_0 = \mathcal{H}_{\text{e}} + \mathcal{H}_{\text{cav}}, \tag{14}$$

we can see that the product states of the adiabatic states $|\psi_\alpha\rangle$ and photon number states $|m\rangle$ are appropriate zeroth-order states states satisfying

$$\mathcal{H}_0|\psi_N^{(0)}\rangle = E_N^{(0)}|\psi_N^{(0)}\rangle \tag{15}$$

with $|\psi_N^{(0)}\rangle = |\psi_{\mu_N}\rangle \otimes |m_N\rangle$ and $E_N^{(0)} = E_{\mu_N} + m_N(\omega + \frac{1}{2})$. In this notation, we are using Greek letters subscripted by upper-case Roman letters (e.g. μ_N) to label the electronic contribution to the zeroth-order product state N, and lower-case Roman letters subscripted by upper-case Roman letters (e.g. m_N) to label the photonic contribution to the zeroth-order product state N. It follows then that the perturbation can be regarded as

$$\mathcal{H}^{'} = \mathcal{H}_{\text{blc}} + \mathcal{H}_{\text{dse}}, \tag{16}$$

so that we can write the total the perturbative expansion of the Pauli-Fierz or coherent state Hamiltonian as

$$\mathcal{H} = \mathcal{H}_0 + \epsilon\mathcal{H}^{'}. \tag{17}$$

Using this partitioning, we can derive perturbative energy corrections with and without application of the coherent state transformation and compare these corrections for the same coupling parameters.

The first order energy correction for then Pauli-Fierz Hamiltonian is

$$\begin{aligned} E^{(1)}_{\text{N,PF}} &= \langle\psi_N^{(0)}|\mathcal{H}^{'}|\psi_N^{(0)}\rangle \\ &= \langle\psi_N^{(0)}|\mathcal{H}_{\text{PF,dse}}|\psi_N^{(0)}\rangle \\ &= \frac{1}{2}\sum_{\gamma} d_{\mu_N\gamma} d_{\gamma\mu_N}, \end{aligned} \tag{18}$$

and the first order energy correction for the coherent state Hamiltonian is

$$\begin{aligned} E^{(1)}_{\text{N,CS}} &= \langle\psi_N^{(0)}|\mathcal{H}^{'}|\psi_N^{(0)}\rangle \\ &= \langle\psi_N^{(0)}|\mathcal{H}_{\text{CS,dse}}|\psi_N^{(0)}\rangle \\ &= \frac{1}{2}\sum_{\gamma} d_{\mu_N\gamma} d_{\gamma\mu_N} - \langle\hat{d}\rangle_0 d_{\mu_N\mu_N} + \frac{1}{2}\langle\hat{d}\rangle_0^2. \end{aligned} \tag{19}$$

The bilinear coupling term does not contribute to the first order correction since the bra and ket have the same photon occupation state.

The second order correction to Pauli-Fierz energy is given as

$$\begin{aligned} E^{(2)}_{\text{N,PF}} &= \sum_{M\neq N} \frac{|\langle\psi_M^{(0)}|\mathcal{H}^{'}|\psi_N^{(0)}\rangle|^2}{E_N^{(0)} - E_M^{(0)}} \\ &= \sum_{M\neq N} \frac{|\langle\psi_M^{(0)}|\mathcal{H}_{\text{PF,blc}}|\psi_N^{(0)}\rangle|^2}{E_N^{(0)} - E_M^{(0)}} + \frac{|\langle\psi_M^{(0)}|\mathcal{H}_{\text{PF,dse}}|\psi_N^{(0)}\rangle|^2}{E_N^{(0)} - E_M^{(0)}} \\ &= \frac{\omega}{2}\sum_{\mu_M} \frac{|d_{\mu_M\mu_N}\sqrt{m_N + 1}|^2}{E_{\mu_N} - E_{\mu_M} - \omega\hbar} \\ &+ \frac{\omega}{2}\sum_{\mu_M} \frac{|d_{\mu_M\mu_N}\sqrt{m_N}|^2}{E_{\mu_N} - E_{\mu_M} + \omega\hbar} \\ &+ \frac{1}{4}\sum_{\mu_M\neq\mu_N} \frac{|\sum_\gamma d_{\mu_M\gamma} d_{\gamma\mu_N}|^2}{E_{\mu_N} - E_{\mu_M}}. \end{aligned} \tag{20}$$

In this case, both the bilinear coupling and the dipole self energy terms contribute to the second order energy correction, but we note that the second line of Equation 20 does not contain cross-terms between the dipole self energy and the bilinear coupling because the former can only contribute when the bra and the ket have the same photon occupation number, and the latter only contributes when the bra and ket differ by one photon occupation number. Similarly, for the second-order correction to the coherent state energy contains both bilinear coupling and dipole self energy terms, and the cross terms between them vanish as well. Here we will expand out these contributions separately first as

$$\begin{aligned} E^{(2)}_{\text{N,CS blc}} &= \sum_{M\neq N} \frac{|\langle\psi_M^{(0)}|\mathcal{H}_{\text{CS,blc}}|\psi_N^{(0)}\rangle|^2}{E_N^{(0)} - E_M^{(0)}} \\ &= \frac{\omega}{2}\sum_{\mu_M} \frac{\left|\left(d_{\mu_M\mu_N} - \langle\hat{d}\rangle_0\delta_{\mu_M\mu_N}\right)\sqrt{m_N + 1}\right|^2}{E_{\mu_N} - E_{\mu_M} - \omega\hbar} \\ &+ \frac{\omega}{2}\sum_{\mu_M} \frac{\left|\left(d_{\mu_M\mu_N} - \langle\hat{d}\rangle_0\delta_{\mu_M\mu_N}\right)\sqrt{m_N}\right|^2}{E_{\mu_N} - E_{\mu_M} + \omega\hbar} \end{aligned} \tag{21}$$

for the bilinear coupling, and

$$E^{(2)}_{\mathrm{N,CS\ dse}} = \sum_{M\neq N} \frac{|\langle\psi_M^{(0)}|\mathcal{H}_{\mathrm{CS,dse}}|\psi_N^{(0)}\rangle|^2}{E_N^{(0)} - E_M^{(0)}} = \frac{1}{4}\sum_{\mu_N\neq\mu_N} \frac{\left|\sum_\gamma d_{\mu_M\gamma}d_{\gamma\mu_N} - \langle\hat{d}\rangle_0 d_{\mu_M\mu_N}\right|^2}{E_{\mu_N} - E_{\mu_M}} \tag{22}$$

for the dipole self energy.

The third order corrections can be written generically as

$$E^{(3)}_{\mathrm{N}} = \sum_{P,Q\neq N} \frac{\langle\psi_N^{(0)}|\mathcal{H}^{'}|\psi_P^{(0)}\rangle\langle\psi_P^{(0)}|\mathcal{H}^{'}|\psi_Q^{(0)}\rangle\langle\psi_Q^{(0)}|\mathcal{H}^{'}|\psi_N^{(0)}\rangle}{(E_N^{(0)} - E_P^{(0)})(E_N^{(0)} - E_Q^{(0)})} - \langle\psi_N^{(0)}|\mathcal{H}^{'}|\psi_N^{(0)}\rangle \sum_{M\neq N} \frac{|\langle\psi_M^{(0)}|\mathcal{H}^{'}|\psi_N^{(0)}\rangle|^2}{(E_N^{(0)} - E_M^{(0)})^2}. \tag{23}$$

We provide more detailed expressions for the third order corrections, as well as ways to factorize the evaluation of these terms, in the Supporting Information.

We can see in the above expressions that the coherent state transformation introduces offsets to the matrix elements that arise in the perturbative corrections, particularly along the diagonal elements of these corrections. This raises the question of if these offsets will reduce the magnitude of the perturbative corrections, yielding a perturbative series that is well behaved for a larger range of ϵ? We will investigate this question numerically in the results section.

2. Perturbation Theory for Cavity Photon

We can take a slightly different perspective than in Section II 1 and consider the matter subsystem to provide a perturbation on the cavity mode. Here will define the zeroth order Hamiltonian as only the bare cavity Hamiltonian, and will consider the perturbation as arising strictly through the bilinear coupling. This will provide insight into the convergence of the photonic subspace in practical coupled calculations.

The bare cavity Hamiltonian can be written as

$$\hat{H}_{0,\mathrm{cav}} = \frac{1}{2}\hat{p}^2 + \frac{1}{2}\omega^2\hat{q}^2 = \hbar\omega\left(\hat{b}^\dagger\hat{b} + \frac{1}{2}\right), \tag{24}$$

where $\hat{p}$ and $\hat{q}$ were defined in Eq. 3. Recalling the definitions of $\hat{d} = \boldsymbol{\lambda}\cdot\hat{\mu}$ where $\boldsymbol{\lambda} = \sqrt{\frac{1}{\epsilon_0 V}}\hat{\mathbf{e}}$, we can express the bilinear coupling as

$$\hat{H}_{\mathrm{blc}} = -\sqrt{\frac{\omega}{2}}\hat{d}\left(\hat{b}^\dagger + \hat{b}\right) = -\omega\hat{d}\hat{q}. \tag{25}$$

We can now take the point of view that the matter perturbs the cavity Hamiltonian through the bilinear coupling term. In this point of view, the bare cavity Hamiltonian can be used as the zeroth order Hamiltonian satisfying the eigenvalue equation

$$\hat{H}_{0,\mathrm{cav}}|n^{(0)}\rangle = E_n^{(0)}|n^{(0)}\rangle = \hbar\omega(n + \frac{1}{2})|n^{(0)}\rangle, \tag{26}$$

and the bilinear coupling term can be the perturbation. The perturbed Hamiltonian for the cavity mode interacting with a polarized matter subsystem can then be written as

$$\begin{aligned}
\hat{H}_{\mathrm{cav}} &= \hat{H}_{0,\mathrm{cav}} + \hat{H}_{\mathrm{blc}} \\
\hat{H}_{\mathrm{cav}} &= \frac{1}{2}\hat{p}^2 + \frac{1}{2}\omega^2\hat{q}^2 - \omega\hat{d}\hat{q} \\
\hat{H}_{\mathrm{cav}} &= \frac{1}{2}\hat{p}^2 + \frac{1}{2}\left(\omega\hat{q} - \hat{d}\right)^2 - \frac{1}{2}\hat{d}^2 \\
\hat{H}_{\mathrm{cav}} &= \hbar\omega\left(\hat{b}^\dagger\hat{b} + \frac{1}{2}\right) - \sqrt{\frac{\omega}{2}}\hat{d}\left(\hat{b}^\dagger + \hat{b}\right).
\end{aligned} \tag{27}$$

The perturbation contains a product of $\hat{d}$ and $\hat{q}$, where the former is a matter operator and the latter a photon operator. The exact eigenstates of this Hamiltonian will self-consistently balance the impact of the photon field on the charges in the matter subsystem and the polarization of the photon field by the charges in the matter subsystem. If, however, we replace the operator $\hat{d}$ with an expectation value $\langle\hat{d}\rangle$ representing the average polarization of the charges in the matter subsystem subject to the photon field, an intuitive picture arises for the photon field subject to an effective potential that arises from the polarized matter. Here, we can look specifically at the third line of Eq. 27 and integrate over the electronic degrees of freedom:

$$\hat{H}_{\mathrm{cav}} = \frac{1}{2}\hat{p}^2 + \frac{1}{2}\left(\omega\hat{q} - \langle\hat{d}\rangle\right)^2 - \frac{1}{2}\langle\hat{d}\rangle^2, \tag{28}$$

where $\langle\hat{d}\rangle$ in an expectation value in terms of an exact electronic eigenstate of the coupled system, which of course is not typically known *a priori*. We can see that this is simply the original cavity Hamiltonian displaced from equilibrium by $\langle\hat{d}\rangle$ and with the total energy shifted by the constant $-\frac{1}{2}\langle\hat{d}\rangle^2$. This shifted Hamiltonian will have the same spectrum of eigenstates as the original Hamiltonian save for a constant shift of all eigenvalues by $-\frac{1}{2}\langle\hat{d}\rangle^2$.

Here we will use perturbative analysis to elucidate how the coherent state transformation can accelerate the convergence of practical calculations of the eigenstates of the Pauli-Fierz Hamiltonian where one generally takes as the basis the photon number states that are eigenstates of the zeroth-order Hamiltonian. Although the shapes of these zeroth-order states match those of the eigenstates of the perturbed Hamiltonian, it will require an expansion of a number of these zeroth-order functions to reproduce the perturbed eigenstates, and this number will increase with the magnitude of the displacement of the potential that goes as $\langle \hat{d} \rangle$.

In particular, let's consider the first and second order correction to photonic state $|n\rangle$:

$$|n^{(1)}\rangle = -\sum_{m \neq n} \frac{\langle m^{(0)}|\omega \langle \hat{d} \rangle \hat{q}|n^{(0)}\rangle}{E_n^{(0)} - E_m^{(0)}} |m^{(0)}\rangle$$

$$|n^{(2)}\rangle = \sum_{k \neq n} \sum_{n \neq n} \frac{\langle k^{(0)}|\omega \langle \hat{d} \rangle \hat{q}|m^{(0)}\rangle \langle m^{(0)}|\omega \langle \hat{d} \rangle \hat{q}|n^{(0)}\rangle}{(E_n^{(0)} - E_m^{(0)})(E_n^{(0)} - E_k^{(0)})} |k^{(0)}\rangle. \tag{29}$$

We note that the position operator $\hat{q}$ can only couple adjacent zeroth-order states, that is, only $\langle n^{(0)}|\hat{q}|(n \pm 1)^{(0)}\rangle$ are non-zero. However, we have a contribution to the first order correction to state $|n\rangle$ that scales linearly with $\omega\langle \hat{d} \rangle$ and couples to states adjacent to $|n\rangle$. The second order correction scales quadratically with $\omega\langle \hat{d} \rangle$ and brings in coupling to states with $|(n \pm 1)\rangle$ and $|(n \pm 2)\rangle$. This trend will continue to higher orders of correction to the states, and is illustrative that for large values of $\omega\langle \hat{d} \rangle$, it will become very difficult to practically converge calculations using the zeroth-order photon basis. This echos the numerical findings of DePrince and co-workers[36] and Vu *et al.*[41] who found that large numbers of photon number states were required to converge variational calculations for polar molecules with strong coupling and for charged molecules under displacements from the origin, both circumstances where $\langle \hat{d} \rangle$ can become large. We will see that application of the coherent state transformation can, at least in certain cases, diminish the magnitude of the couplings that necessitate these corrections. We have also observed that the coherent state transformation can render ai-QED methods manifestly origin invariant for charged molecules, and we can examine these perturbative corrections to examine how this arises.

We can view the coherent state transformation as applying shift to the position coordinate as follows:

$$\hat{U}_{\rm CS}\, \hat{q}\, \hat{U}_{\rm CS}^{\dagger} = \hat{q} + \frac{\langle \hat{d} \rangle_0}{\omega}, \tag{30}$$

so that we can view the coherent state transformed Hamiltonian for the cavity coupled to polarized matter as

$$\hat{U}_{\rm CS} \hat{H}_{\rm cav} \hat{U}_{\rm CS}^{\dagger} = \frac{1}{2}\hat{p}^2 + \frac{1}{2}\left(\omega \hat{q} + \langle \hat{d} \rangle_0 - \hat{d}\right)^2 - \frac{1}{2}\hat{d}^2. \tag{31}$$

If we again average over the electronic degrees of freedom in the coherent state transformed cavity Hamiltonian, then Eq. 32 becomes

$$\hat{U}_{\rm CS} \hat{H}_{\rm cav} \hat{U}_{\rm CS}^{\dagger} \approx \frac{1}{2}\hat{p}^2 + \frac{1}{2}\left(\omega \hat{q} + \langle \hat{d} \rangle_0 - \langle \hat{d} \rangle\right)^2 - \frac{1}{2}\langle \hat{d} \rangle^2 \tag{32}$$

which un-shifts the potential to within the difference between the expectation value of $\langle \hat{d} \rangle_0$ evaluated with a specific reference function and the exact expectation values $\langle \hat{d} \rangle$, which we will denote $\delta_{\langle d \rangle} = \langle \hat{d} \rangle - \langle \hat{d} \rangle_0$. Inserting the same relationship into the perturbative correction to the states yields

$$|n^{(1)}\rangle = -\sum_{m \neq n} \frac{\langle m^{(0)}|\omega \delta_{\langle d \rangle} \hat{q}|n^{(0)}\rangle}{E_n^{(0)} - E_m^{(0)}} |m^{(0)}\rangle$$

$$|n^{(2)}\rangle = \sum_{k \neq n} \sum_{m \neq n} \frac{\langle k^{(0)}|\omega \delta_{\langle d \rangle} \hat{q}|m^{(0)}\rangle \langle m^{(0)}|\omega \delta_{\langle d \rangle} \hat{q}|n^{(0)}\rangle}{(E_n^{(0)} - E_m^{(0)})(E_n^{(0)} - E_k^{(0)})} |k^{(0)}\rangle. \tag{33}$$

Thus, while the perturbative corrections in Eq. 29 scale as orders of $\omega\langle \hat{d} \rangle$, the corrections in Eq. 33 scale as orders of $\omega\delta_{\langle \hat{d} \rangle}$, which will tend to be small as long as the cavity coupling does not lead to changes to the molecular dipole moment that are larger than the uncoupled dipole moment itself.

To see how the coherent state transformation imparts origin invariance, recall that $\hat{d}$ is defined as the lambda vector dotted into the dipole, $\hat{d} = \lambda \cdot \hat{\mu}$, where the dipole operator $\hat{\mu} = \sum_i z_i r_i$, so we can rewrite $\hat{d} = \lambda \cdot \sum_i z_i r_i$. The expectation value is then defined as $\langle \hat{d} \rangle = \lambda \cdot \sum_i z_i \langle \psi | r_i | \psi \rangle$ where ψ is the electronic contribution to the target eigenstate which is unaffected by the coherent state transformation since $\hat{U}_{\rm CS}$ acts only on photonic coordinates. While $\hat{d}$ itself is not origin invariant if the molecule has net charge, $\delta_{\langle d \rangle}$ is origin invariant. To see this, we will consider the expectation value $\langle \hat{d}' \rangle$ following displacement by Δr:

$$\begin{aligned}\langle \hat{d}' \rangle &= \lambda \cdot \left(\sum_i z_i (\langle \psi | r_i | \psi \rangle + \Delta r) \right) \\ &= \langle \hat{d} \rangle + \lambda \cdot \Delta r \sum_i z_i,\end{aligned} \tag{34}$$

which shows that $\langle \hat{d} \rangle$ is itself origin dependent. Similarly, we will write $\langle \hat{d}' \rangle_0$ following displacement by the same Δr as

$$\begin{aligned}\langle \hat{d}' \rangle_0 &= \lambda \cdot \left(\sum_i z_i (\langle \Phi_0 | r_i | \Phi_0 \rangle + \Delta r) \right) \\ &= \langle \hat{d} \rangle_0 + \lambda \cdot \Delta r \sum_i z_i,\end{aligned} \tag{35}$$

so that we see $\langle \hat{d} \rangle_0$ has the same origin dependence. Finally, we consider $\delta_{\langle d' \rangle}$,

$$\begin{aligned}\delta_{\langle d' \rangle} &= \langle \hat{d} \rangle + \lambda \cdot \Delta r \sum_i z_i - \langle \hat{d} \rangle_0 - \lambda \cdot \Delta r \sum_i z_i \\ &= \langle \hat{d} \rangle - \langle \hat{d} \rangle_0,\end{aligned} \tag{36}$$

which is origin invariant.

III. COMPUTATIONAL DETAILS

We formulate perturbative corrections to Pauli-Fierz and coherenst state transformed Hamiltonians projected onto a subspace of adiabatic many-electron states and photonic Fock states. The adiabatic many-electron states are computed using full configuration interaction (FCI) using the qed-ci package[66] which interfaces with the psi4 package for standard electron integrals.[67,68] We take variational calculations of the projected Pauli-Fierz Hamiltonian in a sufficiently large basis of electronic and photonic states (herein referred to as variational pQED) to be the numerically exact answer and compare the perturbative corrections to this variational calculation in all cases. All variational and perturbative calculations are also performed using the qed-ci package. We apply these approaches to the helium hydride cation (HeH^+), lithium hydride (LiH), and hydroxide anion (OH^-). We represent the HeH^+ system in the cc-pVQZ[69] (results from cc-pVDZ and cc-pVTZ are shown in the Supporting Information), we represent LiH in a 6-311G basis set[70], and OH^- in a 6-31G basis set. For all variational calculations, we consider a photonic Fock space with 10 number states ($|0\rangle, |1\rangle, ..., |9\rangle$); these details are summarized in Table I. A glossary of acronyms used in describing the various perturbative and variational approaches is provided in Table II.

System	Orbital Basis	N_{el}	N_{p}
HHe^+	cc-pVQZ	2880	10
LiH	6-311g	500	10
OH^-	6-31G	50	10

TABLE I. Summary of the orbital basis, size of the adiabatic many-electron basis, and (for variational calculations) size of the photonic Fock state basis for calculations presented in the results section.

pQED(N_{el}, N_{p})	Variational solution of Eq. 1 projected onto a basis of N_{el} adiabatic many electron states and N_{p} photonic Fock states
PF-PT2(N_{el})	Second order perturbative approximation to Eq. 1 projected onto a basis of N_{el} adiabatic many electron states
PF-PT3(N_{el})	Third order perturbative approximation to Eq. 1 projected onto a basis of N_{el} adiabatic many electron states
CS-PT2(N_{el})	Second order perturbative approximation to Eq. 5 projected onto a basis of N_{el} adiabatic many electron states
CS-PT3(N_{el})	Third order perturbative approximation to Eq. 5 projected onto a basis of N_{el} adiabatic many electron states

TABLE II. Glossary of acronyms used to describe different methodologies used in this work.

IV. RESULTS

We provide several illustrative numerical examples of the behavior of the coherent state transformation following the discussion in Sections II 1 and II 2. Specifically, to illustrate the discussion in Section II 1, we will consider the second- and third-order perturbative corrections to the ground state energy of the helium hydride ion and the lithium hydride molecule. In both cases, we will compare the resulting ground state estimates to the variational result that we obtain after projecting the Pauli-Fierz Hamiltonian onto a very large subspace of electronic states and photonic states, which we will take to be the exact ground state of the projected Pauli-Fierz Hamiltonian. The orbital, many-electron, and photonic Fock basis details for each system are provided in Section III.

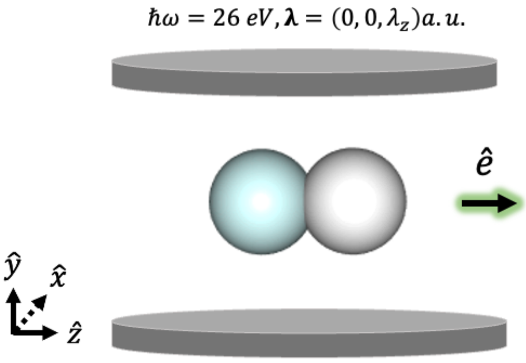

FIG. 1. Schematic of the HeH^+ coupled to a cavity mode polarized along the internuclear axis (z) and tuned to the first optically allowed transition from $S_0 \rightarrow S_2$ at approximately 26 eV.

A. Peturbation theory for the coupled ground state

1. Helium hydride cation

We first consider HeH^+ cation coupled to a cavity mode resonant with the first dipole allowed transition ($S_0 \rightarrow S_2$) which has a transition dipole moment oriented along the inter-nuclear axis (the z-axis in Figure 1). We fix the geometry at the equilibrium bond length found at the (cavity free) FCI/cc-pVTZ level, which is 0.77 Angstroms. At this geometry, the ground state has a permanent dipole moment of 1.73 Debye along the z axis, and the $S_0 \rightarrow S_2$ transition energy has an energy of 26.1 eV. We fix the energy of the cavity mode to be on resonance with this transition and consider values λ_z ranging from 0 to 0.1 atomic units. Although these coupling conditions can lead to the formation of polariton states, in this work we focus exclusively on the ground state of the coupled system. Degenerate perturbation theory is required to resolve the degeneracies that will arise when polariton states are targetted, and will be the subject of future work.

The behaviour of the ground-state energies to second and third-order of perturbation theory to Eq. 1 (PF-PT2(2880)/cc-pVQZ and PF-PT3(2880)/cc-pVQZ) and

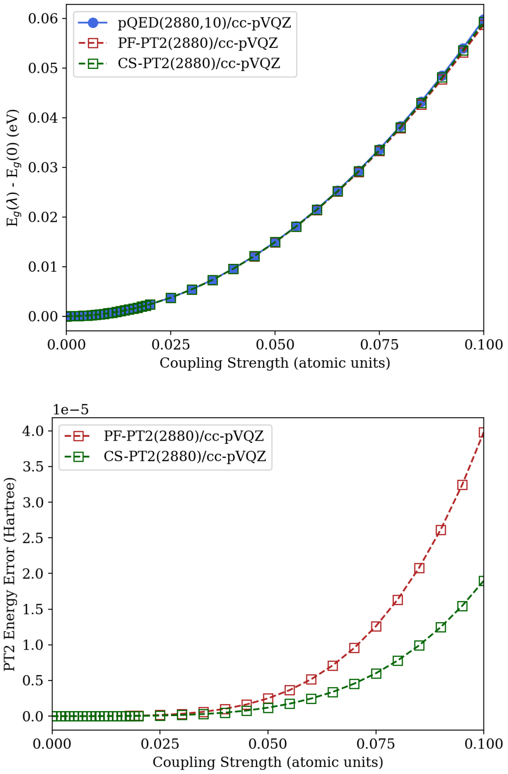

FIG. 2. Ground state energy from second-order perturbation theory for HeH$^+$ coupled to a cavity photon with $\hbar\omega = 26$ eV across a range of coupling strengths. (Top) Relative energy of the coupled ground state as a function of coupling strength as computed by a fully-converged variational approach to the Pauli-Fierz Hamiltonian and by second-order perturbation theory for the Pauli-Fierz and coherent state Hamiltonians. (Bottom) Error of second-order perturbation theory for the PF and CS Hamiltonians relative to the fully-converged variational calculation as a function of coupling strength.

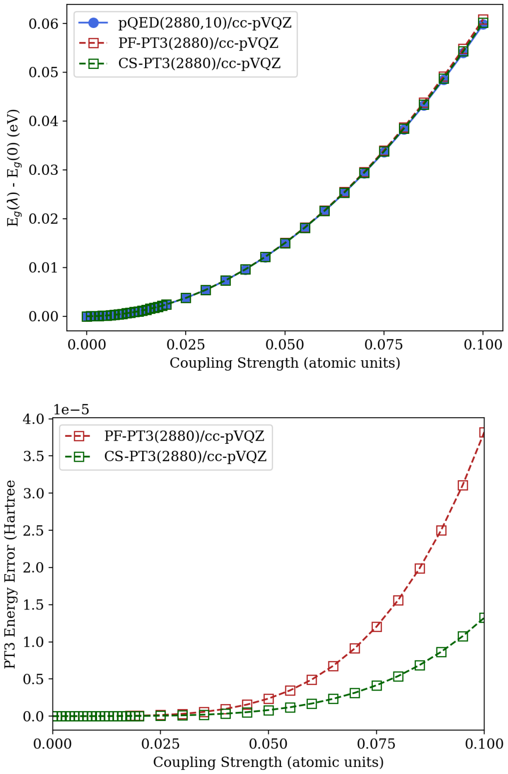

FIG. 3. Ground state energy from second-order perturbation theory for HeH$^+$ coupled to a cavity photon with $\hbar\omega = 26$ eV across a range of coupling strengths. (Top) Relative energy of the coupled ground state as a function of coupling strength as computed by a fully-converged variational approach to the Pauli-Fierz Hamiltonian and by third-order perturbation theory for the Pauli-Fierz and coherent state Hamiltonians. (Bottom) Error of third-order perturbation theory for the PF and CS Hamiltonians relative to the fully-converged variational calculation as a function of coupling strength.

Eq. 5 (CS-PT2(2880)/cc-pVQZ and CS-PT3(2880)/cc-pVQZ) are shown in Figures 2 and 3, with errors reported relative to the exact variational ground state computed at the pQED(2880,10)/cc-pVQZ level. In the top panel of 2, we have $E_g(\lambda) - E_g(0)$ plotted versus coupling strength, where $E_g(\lambda)$ is the energy of the coupled system with λ representing the coupling strength, and $E_g(0)$ is the energy of the uncoupled system. This plot shows the exact $E_g(\lambda) - E_g(0)$ from pQED(2880,10)/cc-pVQZ and the CS and PF formulations of second-order perturbation theory. The energy of the system increases as coupling between the molecule and the cavity increases, thus, the size of the perturbation is also increasing. We observe that both PT2 results have negligible error when the coupling strength is less than $\lambda_z \approx 0.025$ atomic units, but starts depart for stronger coupling (see Figure 2 bottom panel). At the larger values of λ_z, CS-PT2 has a consistently smaller error compared to PF-PT2. The top panel of Figure 3 is similar to Figure 2 except the former now has the third-order perturbative approximations to pQED. Again, we see that the CS-PT3 and PF-PT3 energies have negligible error for small coupling strength, and again start to depart for values of lambda larger than $\lambda_z \approx 0.025$ atomic units, and again, CS-PT3 has consistently smaller errors than the PF-PT3 results (see Figure 3 bottom panel).

2. Lithium hydride bond stretch

The LiH ground state potential energy surface is computed between bond lengths of 1.4 and 2.2 angstroms coupled to a cavity mode with frequency $\hbar\omega_{\text{cav}} = 3.28$ eV polarized along the z-axis with $\lambda_z = 0.05$ atomic units (see Figure 4). We compare PF-PT2(500)/6-311G and CS-PT2(500)/6-311G to exact variational potential energy surface (pQED(500,10)/6-311G) in Figure 5, and the PT3 analogs are compared to the exact variational potential energy surface in Figure 6.

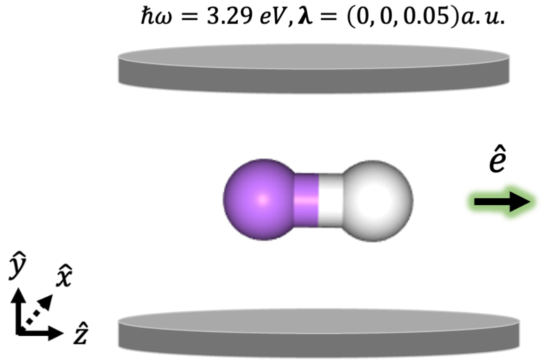

FIG. 4. Schematic of the LiH coupled to a cavity mode polarized along the internuclear axis (z) and tuned to the first optically allowed transition from $S_0 \rightarrow S_1$ at approximately 3.29 eV.

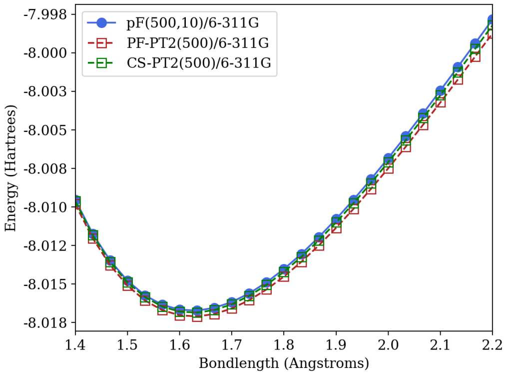

FIG. 5. Ground state potential energy surface for LiH coupled to a cavity photon with $\hbar\omega = 3.28$ eV across a range of r values with a coupling strength of 0.05 au. Relative energy of the coupled ground state as a function of bond length computed by a fully-converged variational approach to the Pauli-Fierz Hamiltonian and by second-order perturbation theory for the Pauli-Fierz and coherent state Hamiltonians.

Level of Theory	Root Mean Squared Error (Hartrees)
PF-PT2(500)	$5.58 \cdot 10^{-4}$
PF-PT3(500)	$5.97 \cdot 10^{-4}$
CS-PT2(500)	$2.18 \cdot 10^{-4}$
CS-PT3(500)	$2.36 \cdot 10^{-4}$

TABLE III. Comparison of mean squared errors for different levels of theory for the LiH PES under strong coupling. Errors calculated with respect to pQED(500,10)

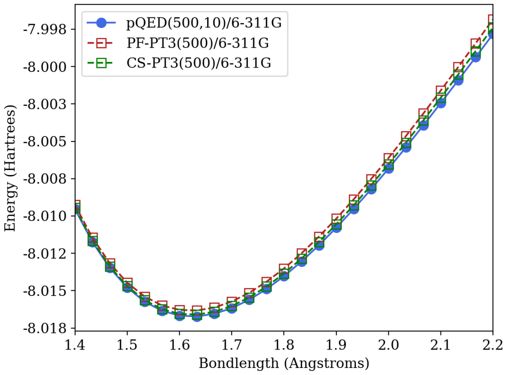

FIG. 6. Ground state potential energy surface for LiH coupled to a cavity photon with $\hbar\omega = 3.28$ eV across a range of r values with a coupling strength of 0.05 au. Relative energy of the coupled ground state as a function of bond length computed by a fully-converged variational approach to the Pauli-Fierz Hamiltonian and by third-order perturbation theory for the Pauli-Fierz and coherent state Hamiltonians.

As with the HHe+ system, the CS-PTn results are consistently closer to the numerically exact pQED results as compared to PF-PTn results. It can be seen in Figure 5 that the CS-PT2 and PF-PT2 curves are both lower bounds to the exact variational curve, with the CS-PT2 being closer across the stretch. Furthermore, we see in Figure 6 that the CS-PT3 and PF-PT3 curves are upper bounds to the exact curve, with the CS-PT3 being closer to the variational curve across the stretch. In Table III, the root mean squared (RMS) error between the perturbative approaches and the pQED across the bond length scan are reported. Interestingly, we see the CS-PT2 result has the smallest RMS error. While the CS-PT3 RMS error is smaller than the PF-PT3 RMS error, we observe that the PF-PT3 RMS error is slightly larger than the PF-PT2 error just as the CS-PT3 RMS error is slightly larger than the CS-PT2 RMS error. Plots of magnitude and relative errors for the perturbative approaches vs. pQED(500,10)/6-311G are shown in the Supporting Information for λ_z values of 0.01 and 0.05 in Figures S5 and S6, respectively. The trajectories of the errors shown in Figures S5 and S6 show a systematic increase with increasing bond length, suggesting the magnitude of the light-matter coupling increases similarly. This is likely attributable to the monotonic increases in the magnitude of the dipole moment as the LiH bond is stretched (see Figure S7). In particular, the dipole self energy term increases quadratically with the permanent dipole, and so this scaling will tend to dominate the magnitude of the perturbation. An important requirement for the validity of perturbation theory is that the magnitude of the perturbation be relatively small, and failure of this criteria leads to non-convergent perturbative series where subsequent orders of perturbation theory take one further away, rather than closer, to the exact answer. Figure S5 reveals that when $\lambda_z = 0.01$, the magnitude of the error of PF-PT3 exceeds the error of PF-PT2 for values of the LiH bond length greater than about 1.8 Angstroms where the ground-state dipole has a magnitude greater than 2.35 Debye. Interestingly, the CS-PT3 error is consistently smaller than the CS-PT2 error across the stretch when $\lambda_z = 0.01$ atomic units. When we observe the analogous behavior with a larger coupling strength ($\lambda_z = 0.05$

atomic units), we see that the PF-PT3 error is larger than the PF-PT2 error for all value of the bond length, whereas the CS-PT3 error only exceeds the CS-PT2 error for bond lengths greater than about 1.8 Angstroms. These results are consistent with the supposition that the coherent state transformation can mitigate the light-matter coupling and extend the perturbative regime for these coupled systems.

B. Perturbation theory for the cavity ground state

To investigate the impact of the coherent state transformation on the convergence of the photonic subspace, we consider two examples of the matter subsystem perturbing the cavity Hamiltonian. In the first example, we revisit the lithium hydride system as an example of a polar molecule that can strongly perturb the cavity Hamiltonian through bilinear coupling, and we illustrate how the coherent state transformation can effectively mitigate this perturbation. In the second example, we consider the hydroxide anion as a charged species that has an origin-dependent dipole moment. This property of charged species can induce very large perturbations to cavity modes when the molecule is displaced away from the cavity origin, and in the un-transformed representation, can impart a strong origin dependence in the energy that necessitates a large photonic Fock spaces to numerically resolve.

1. Lithium Hydride

We again consider the LiH molecule within the 6-311G basis set with a bond length of 1.55 Angstroms coupled to a photon with frequency $\hbar\omega_{\rm cav} = 3.28$ eV (0.1208 Hartrees) polarized along the z-axis with $\lambda_z = 0.2$ atomic units. We choose a large value of λ to clearly illustrate the impact of strong coupling on the cavity potential, and the bond length of 1.55 Angstroms was chosen as the equilibrium bond length for these cavity conditions. In the top panel of Figure 7, we illustrate the bare cavity potential given by $V(\hat{q}) = \frac{1}{2}\omega_{\rm cav}^2\hat{q}^2$ in solid black lines, and the perturbed potential given by $V'(\hat{q}) = \frac{1}{2}\omega_{\rm cav}^2\hat{q}^2 - \omega_{\rm cav}\langle\hat{d}\rangle\hat{q}$ in dashed black lines. The large displacement of these potentials is indicative of the magnitude of the cavity polarization imparted by the bilinear coupling to the polar matter subsystem. The expectation value $\langle\hat{d}\rangle$ is computed at the pQED(500,10)/6-311G level and $\langle\hat{d}\rangle_0$ is computed at the FCI/6-311G level (see Section III for more details). We plot the exact ground-state cavity wavefunction for the perturbed system $|0\rangle$ on the perturbed potential (see Figure 7 top panel). Due to the polarization induced by the bilinear coupling, the $|0\rangle$ state has considerable coupling to excited zeroth-order states ($|n^{(0)}\rangle$ with $n > 0$). We capture this coupling through the first- and second-order corrections to state $|0\rangle$ in the top panel of Figure 7, where the contributions $|0^{(1)}\rangle$ and $|0^{(2)}\rangle$ are shown on the unperturbed potential. In particular, these corrections have the explicit form

$$|0^{(1)}\rangle = \frac{\langle\hat{d}\rangle}{\sqrt{2\omega_{\rm cav}}}|1^{(0)}\rangle$$
$$|0^{(2)}\rangle = \frac{\langle\hat{d}\rangle^2}{2\sqrt{2}\omega_{\rm cav}}|2^{(0)}\rangle, \tag{37}$$

where we have evaluated Eq. 29 analytically to obtain these expressions in terms of $\langle\hat{d}\rangle$ and $\omega_{\rm cav}$. Numerical values for the first- and second-order coefficients are provided in Table IV, and we can visually see that there is considerable contribution from the first- and second-order corrections owing to the magnitude of the bilinear coupling term. The bottom panel of Figure 7 illustrate the perturbed potential following coherent state transformation, $\hat{U}_{\rm CS}V'(\hat{q})\hat{U}_{\rm CS}^{\dagger} = \frac{1}{2}(\omega_{\rm cav}\hat{q} + \langle\hat{d}\rangle_0 - \langle\hat{d}\rangle)^2 - \frac{1}{2}\langle\hat{d}\rangle)^2$ in a dashed black line against the unperturbed potential in solid black line, and we again plot the exact state $|0\rangle$ along the transformed perturbed potential and the first- and second-order corrections ($|0^{(1)}\rangle$ and $|0^{(2)}\rangle$) along the unperturbed potential. We can clearly see the impact of the transformation on the location of the minima of the potential, which is now visibly indiscernible from the minima of the unperturbed potential. Similarly, we can see that the first- and second-order corrections to state $|0\rangle$ are vanishingly small following the transformation (see Figure 7 bottom panel). The first- and second-order coefficients can again be evaluated analytically by substituting $\delta_{\langle d\rangle}$ for $\langle\hat{d}\rangle$ in Eqs. 37, and are tabulated in Table IV where we see the first-order coefficient is roughly 75 times smaller in magnitude the second-order coefficient is more than 5000 times smaller in magnitude following the coherent state transformation. This illustrates how the coherent state transformation can effectively mitigate the polarization of the cavity models by polar matter that would typically necessitate a large number of photonic Fock states to recover.

2. Hydroxide anion

To illustrate the ability of the coherent state transformation to ensure numerical origin invariance for energies of charged molecules, we consider the hydroxide anion displaced 20 Angstroms from the cavity origin (see Figure 8). The OH^- anion is represented within the 6-31G basis set with a bond length of 0.9 Angstroms coupled to a photon with frequency $\hbar\omega_{\rm cav} = 5.96$ eV (0.219 Hartrees) polarized along the z-axis with $\lambda_z = 0.05$ atomic units. We note that this field does not couple directly to a transition in the molecule; while there is a dipole allowed transition at 5.96 eV, in this coordinate system, it does not have a transition dipole moment along the polarization axis of the field. Therefore, the coupling occurs through the permanent dipole moment

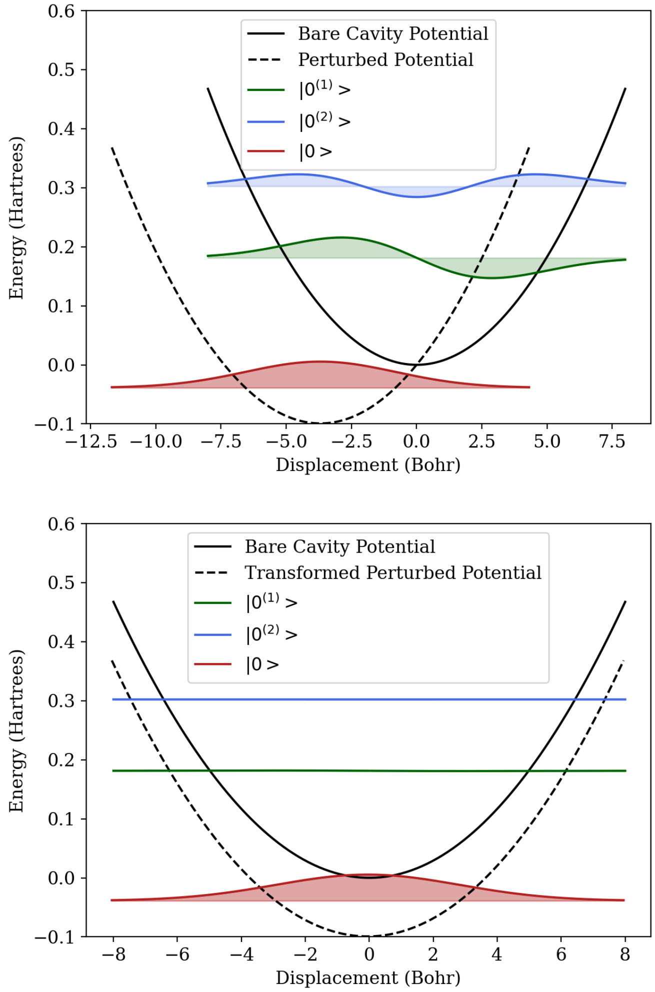

FIG. 7. (Top) Illustration of the polarization of a cavity mode with $\omega_{\text{cav}} = 3.28$ eV through bilinear coupling to the LiH molecule with coupling strength $\lambda_z = 0.2$ atomic units. The unperturbed (solid black) and perturbed (dashed black) potentials are plotted along with the exact ground-state wavefunction for the cavity mode on the perturbed potential, and its first- and second-order corrections on the unperturbed potential. (Bottom) The same system is represented following application of the coherent state transformation to the cavity Hamiltonian.

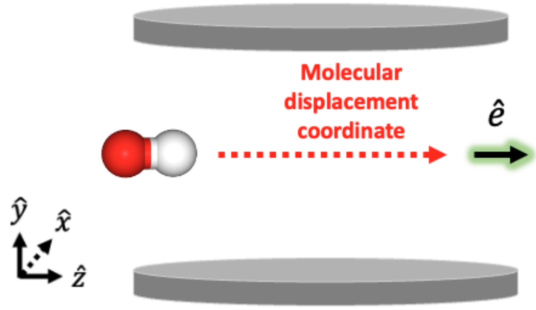

FIG. 8. Schematic of the OH$^-$ displaced from the cavity origin. The cavity mode has energy of $\hbar\omega = 5.96$ eV with $\lambda_z = 0.05$ atomic units, polarized along the internuclear axis of the molecule.

System	Without Transformation		With Transformation	
	$c^{(1)}$	$c^{(2)}$	$c^{(1)}$	$c^{(2)}$
LiH	-9.06 $\cdot 10^{-1}$	5.80 $\cdot 10^{-1}$	-1.24 $\cdot 10^{-2}$	1.08 $\cdot 10^{-4}$
OH$^-$	-2.80 $\cdot 10^{0}$	5.57 $\cdot 10^{0}$	5.11 $\cdot 10^{-4}$	1.85 $\cdot 10^{-7}$

TABLE IV. Coefficients for first- and second-order corrections to the ground state cavity wavefunction for the LiH and displaced OH$^-$ system with and without the coherent state transformation.

of the molecule. The expectation value $\langle \hat{d} \rangle$ is computed at the pQED(50,10)/6-31G level, and $\langle \hat{d} \rangle_0$ is computed at the FCI/6-31G level. The top panel of Figure 9 shows the unperturbed cavity potential (solid black line), the perturbed potential when the molecule is at the cavity origin (dashed-dotted black line), and the perturbed potential when the molecule is displaced by 20 Angstroms from the cavity origin (dashed black line). We can see the profound influence that the origin dependent dipole moments have on the displacement of the perturbed potential. While the perturbed potential from the molecule at the cavity origin is almost indiscernible from the unperturbed potential at this coupling strength, the perturbed potential from the displaced molecule is dramatically displaced. In other words, the hydroxide anion provides some intrinsic polarization of the cavity state, and also has a polarizing effect that is proportional to its displacement from the cavity origin owing to its origin-dependent dipole moment. For this particular system (i.e. the cavity coupling strength and the displacement), the polarization arising from the molecular displacement is much more dramatic. We also see that this polarization imparts even stronger coupling between the ground state wavefunction of the perturbed cavity and excited zeroth-order states (see top panel of Figure 9). However, application of the coherent state transformation completely eliminates the polarization that arises from displacement from the cavity origin, and (similar to what was demonstrated for LiH), results in cavity polarization that is proportional to $\delta_{\langle \hat{d} \rangle}$. Accordingly, we see that the transformed potential aligns closely with the unperturbed potential, and the coupling between the cavity ground state and excited zeroth-order states is almost entirely eliminated (see the bottom panel of Figure 9). In this case, we see even more dramatic reduction in the magnitude of the first- and second-order coefficients following coherent state transformation: the first-order coefficient is more than 5000 times smaller in magnitude and the second-order coefficient is more than 7 orders of magnitude times smaller following the coherent state transformation.

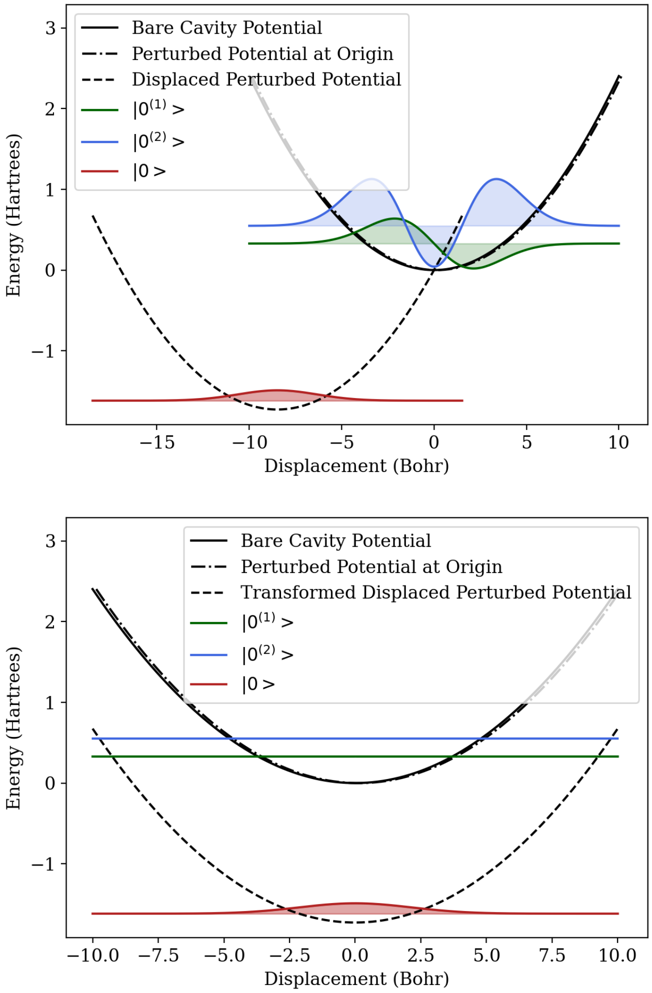

FIG. 9. (Top) Illustration of the polarization of a cavity mode with $\omega_{\text{cav}} = 5.96$ eV through bilinear coupling to the OH$^-$ anion with coupling strength $\lambda_z = 0.05$ atomic units with and without displacement of the anion from the cavity origin. The unperturbed (solid black) and perturbed potentials that arise when the molecule shares the same origin as the cavity (dashed-dotted black) and when it is displaced from the cavity origin (dashed black) are plotted along with the exact ground-state wavefunction for the cavity mode on the perturbed potential, and its first- and second-order corrections on the unperturbed potential. (Bottom) The same system is represented following application of the coherent state transformation to the cavity Hamiltonian.

V. CONCLUDING REMARKS

In this work, we utilized perturbation theory to elucidate favorable computational properties, namely faster convergence of the photonic Fock space and robustly origin-invariant energies, that arise when the coherent state transformation is applied to *ab initio* QED methodologies. In partciular, we found that applying the coherent state transformation yields second- and third-order estimates to the ground state energy that are in consistently better agreement with exact ground state across a range of coupling strengths as compared to the same orders without transformation of the Hamiltonian. We reason that this advantage arises because of the partial decoupling between the light-matter subsystems that arises from this transformation that tends to increase the radius of convergence of the perturbative series. Furthermore, when we treated the bilinear coupling between electron and photon degrees of freedom as a perturbation to the cavity Hamiltonian, we found that the coherent state transformation decouples the systems to within a magnitude that is related to the error in the reference estimate of the dipole moment expectation value that parameterizes the transformation for a target coupled state. We showed that this error is manifestly origin invariant, and so this result sheds light on why the coherent state transformation accelerates photon convergence and restores origin invariance in *ab initio* QED calculations.

Acknowledgments JJF and PR gratefully acknowledge the NSF CAREER Award CHE-2043215 for financial support. JJF gratefully acknowledges UNC Charlotte for startup funds.

Data Availability Open-source implementation of the methods used for the results presented within can be accessed in the following GitHub repository: `https://github.com/mapol-chem/qed-ci/tree/jcp_submission`.

The data that support the findings of this study are available from the corresponding author upon reasonable request; json data corresponding to the results in Section IV.A may be found `https://github.com/FoleyLab/data_repository/`; specifically for HeH$^+$ data here: `https://github.com/FoleyLab/data_repository/tree/main/Mapol/HHep/perturbation_theory` and for LiH data here: `https://github.com/FoleyLab/data_repository/tree/main/Mapol/LiH/perturbation_theory`. An example Jupyter notebook producing the figures and coefficients used in results Section IV B may be found here: `https://github.com/FoleyLab/SCQED-PCQED/blob/perturbation_theory/src/OHminus_PT_for_Cavity.ipynb`.

VI. REFERENCES

[1] A. Frisk Kockum, A. Miranowicz, S. De Liberato, S. Savasta, and F. Nori, "Ultrastrong coupling between light and matter," Nature Reviews Physics **1**, 19–40 (2019).
[2] J. Flick, N. Rivera, and P. Narang, "Strong light-matter coupling in quantum chemistry and quantum photonics," Nanophotonics **7**, 1479 – 1501 (2018).
[3] P. Törmä and W. L. Barnes, "Strong coupling between surface plasmon polaritons and emitters: a review," Reports on Progress in Physics **78**, 013901 (2014).
[4] D. G. Lidzey, D. D. C. Bradley, M. S. Skolnick, T. Virgili, S. Walker, and D. M. Whittaker, "Strong exciton–photon cou-

pling in an organic semiconductor microcavity," Nature **395**, 53–55 (1998).

[5] J. Bellessa, C. Bonnand, J. C. Plenet, and J. Mugnier, "Strong coupling between surface plasmons and excitons in an organic semiconductor," Phys. Rev. Lett. **93**, 036404 (2004).

[6] J. A. Hutchison, T. Schwartz, C. Genet, E. Devaux, and T. W. Ebbesen, "Modifying chemical landscapes by coupling to vacuum fields," Angewandte Chemie International Edition **51**, 1592–1596 (2012).

[7] D. M. Coles, Y. Yang, Y. Wang, R. T. Grant, R. A. Taylor, S. K. Saikin, A. Aspuru-Guzik, D. G. Lidzey, J. K.-H. Tang, and J. M. Smith, "Strong coupling between chlorosomes of photosynthetic bacteria and a confined optical cavity mode," Nature Communications **5**, 5561 (2014).

[8] E. Orgiu, J. George, J. A. Hutchison, E. Devaux, J. F. Dayen, B. Doudin, F. Stellacci, C. Genet, J. Schachenmayer, C. Genes, G. Pupillo, P. Samorì, and T. W. Ebbesen, "Conductivity in organic semiconductors hybridized with the vacuum field," Nature Materials **14**, 1123–1129 (2015).

[9] R. Chikkaraddy, B. de Nijs, F. Benz, S. J. Barrow, O. A. Scherman, E. Rosta, A. Demetriadou, P. Fox, O. Hess, and J. J. Baumberg, "Single-molecule strong coupling at room temperature in plasmonic nanocavities," Nature **535**, 127–130 (2016).

[10] T. W. Ebbesen, "Hybrid light–matter states in a molecular and material science perspective," Accounts of Chemical Research **49**, 2403–2412 (2016).

[11] M. Sukharev and A. Nitzan, "Optics of exciton-plasmon nanomaterials," Journal of Physics: Condensed Matter **29**, 443003 (2017).

[12] X. Zhong, T. Chervy, L. Zhang, A. Thomas, J. George, C. Genet, J. A. Hutchison, and T. W. Ebbesen, "Energy transfer between spatially separated entangled molecules," Angewandte Chemie International Edition **56**, 9034–9038 (2017).

[13] K. Chevrier, J. M. Benoit, C. Symonds, S. K. Saikin, J. Yuen-Zhou, and J. Bellessa, "Anisotropy and controllable band structure in suprawavelength polaritonic metasurfaces," Phys. Rev. Lett. **122**, 173902 (2019).

[14] S. Kéna-Cohen and S. R. Forrest, "Room-temperature polariton lasing in an organic single-crystal microcavity," Nature Photonics **4**, 371–375 (2010).

[15] N. M. Hoffmann, L. Lacombe, A. Rubio, and N. T. Maitra, "Effect of many modes on self-polarization and photochemical suppression in cavities," J. Chem. Phys. **153**, 104103 (2020), https://pubs.aip.org/aip/jcp/article-pdf/doi/10.1063/5.0012723/16726857/104103_1_online.pdf.

[16] A. Mandal and P. Huo, "Investigating new reactivities enabled by polariton photochemistry," The Journal of Physical Chemistry Letters **10**, 5519–5529 (2019).

[17] P. Antoniou, F. Suchanek, J. F. Varner, and J. J. Foley, "Role of cavity losses on nonadiabatic couplings and dynamics in polaritonic chemistry," J. Phys. Chem. Lett. **11**, 9063–9069 (2020).

[18] A. Mandal, M. Taylor, B. Weight, E. Koessler, X. Li, and P. Huo, "Theoretical advances in polariton chemistry and molecular cavity quantum electrodynamics," Chem. Rev. **16**, 9786–9879 (2023).

[19] "Theoretical challenges in polaritonic chemistry," ACS Photonics **9**, 1096–1107 (2022).

[20] A. D. Wright, J. C. Nelson, and M. L. Weichman, "Rovibrational polaritons in gas-phase methane," J. Am. Chem. Soc. **145**, 5982–5987 (2023).

[21] M. Ruggenthaler, F. Mackenroth, and D. Bauer, "Time-dependent Kohn-Sham approach to quantum electrodynamics," Phys. Rev. A **84**, 042107 (2011).

[22] I. V. Tokatly, "Time-dependent density functional theory for many-electron systems interacting with cavity photons," Phys. Rev. Lett. **110**, 233001 (2013).

[23] M. Ruggenthaler, J. Flick, C. Pellegrini, H. Appel, I. V. Tokatly, and A. Rubio, "Quantum-electrodynamical density-functional theory: Bridging quantum optics and electronic-structure theory," Phys. Rev. A **90**, 012508 (2014).

[24] C. Pellegrini, J. Flick, I. V. Tokatly, H. Appel, and A. Rubio, "Optimized effective potential for quantum electrodynamical time-dependent density functional theory," Phys. Rev. Lett. **115**, 093001 (2015).

[25] J. Flick, C. Schäfer, M. Ruggenthaler, H. Appel, and A. Rubio, "Ab initio optimized effective potentials for real molecules in optical cavities: Photon contributions to the molecular ground state," ACS Photonics **5**, 992–1005 (2018).

[26] R. Jestädt, M. Ruggenthaler, M. J. T. Oliveira, A. Rubio, and H. Appel, "Light-matter interactions within the ehrenfest–maxwell–pauli–kohn–sham framework: fundamentals, implementation, and nano-optical applications," Advances in Physics **68**, 225–333 (2019).

[27] J. Flick and P. Narang, "Ab initio polaritonic potential-energy surfaces for excited-state nanophotonics and polaritonic chemistry," J. Chem. Phys. **153**, 094116 (2020).

[28] J. McTague and J. J. Foley IV, "Non-hermitian cavity quantum electrodynamics–configuration interaction singles approach for polaritonic structure with ab initio molecular hamiltonians," J. Chem. Phys. **156**, 154103 (2022).

[29] T. S. Haugland, E. Ronca, E. F. Kjønstad, A. Rubio, and H. Koch, "Coupled cluster theory for molecular polaritons: Changing ground and excited states," Phys. Rev. X **10**, 041043 (2020).

[30] A. E. DePrince III, "Cavity-modulated ionization potentials and electron affinities from quantum electrodynamics coupled-cluster theory," J. Chem. Phys. **154**, 094112 (2021).

[31] U. Mordovina, C. Bungey, H. Appel, P. J. Knowles, A. Rubio, and F. R. Manby, "Polaritonic coupled-cluster theory," Physical Reviews Research **2**, 023262 (2020).

[32] J. Yang, Q. Ou, Z. Pei, H. Wang, B. Weng, Z. Shuai, K. Mullen, and Y. Shao, "Quantum-electrodynamical time-dependent density functional theory within gaussian atomic basis," J. Chem. Phys. **155**, 064107 (2021).

[33] J. Yang, Z. Pei, E. C. Leon, C. Wickizer, B. Weng, Y. Mao, Q. Ou, and Y. Shao, "Cavity quantum-electrodynamical time-dependent density functional theory within Gaussian atomic basis. II. Analytic energy gradient," J. Chem. Phys. **156**, 124104 (2022).

[34] M. L. Vidal, F. R. Manby, and P. J. Knowles, "Polaritonic effects in the vibronic spectrum of molecules in an optical cavity," The Journal of Chemical Physics **156**, 204119 (2022), https://pubs.aip.org/aip/jcp/article-pdf/doi/10.1063/5.0089412/18289379/204119_1_5.0089412.pdf.

[35] N. Vu, G. M. McLeod, K. Hanson, and A. E. I. DePrince, "Enhanced diastereocontrol via strong light–matter interactions in an optical cavity," J. Phys. Chem. A **126**, 9303–9312 (2022).

[36] J. J. Foley IV, J. McTague, and A. E. DePrince III, "*Ab initio* methods for polariton chemistry," Chem. Phys. Rev **4**, 041301 (2023).

[37] M. D. Liebenthal, N. Vu, and A. E. DePrince III, "Assessing the effects of orbital relaxation and the coherent-state transformation in quantum electrodynamics density functional and coupled-cluster theories," J. Phys. Chem. A **127**, 5264–5275 (2023).

[38] M. Bauer and A. Dreuw, "Perturbation theoretical approaches to strong light–matter coupling in ground and excited electronic states for the description of molecular polaritons," J. Chem. Phys. **158**, 124128 (2023), https://pubs.aip.org/aip/jcp/article-pdf/doi/10.1063/5.0142403/16794111/124128_1_online.pdf.

[39] D. Hu and P. Huo, "Ab initio molecular cavity quantum electrodynamics simulations using machine learning models," J. Chem. Theory. Comput. **19**, 2353–2368 (2023), pMID: 37000936.

[40] B. M. Weight, T. D. Krauss, and P. Huo, "Investigating molecular exciton polaritons using ab initio cavity quantum electrodynamics," J. Phys. Chem. Lett. **14**, 5901–5913 (2023), pMID: 37343178.

[41] N. Vu, D. Mejia-Rodriguez, N. P. Bauman, A. Panyala, E. Mutlu, N. Govind, and J. J. I. Foley, "Cavity quantum electrodynamics complete active space configuration interaction theory," Journal of Chemical Theory and Computation **20**, 1214–1227 (2024),

pMID: 38291561, https://doi.org/10.1021/acs.jctc.3c01207.

[42] B. M. Weight, S. Tretiak, and Y. Zhang, "Diffusion quantum monte carlo approach to the polaritonic ground state," Phys. Rev. A **109**, 032804 (2024).

[43] Z.-H. Cui, A. Mandal, and D. R. Reichman, "Variational lang–firsov approach plus møller–plesset perturbation theory with applications to ab initio polariton chemistry," J. Chem. Theory Comput. **20**, 1143 (2024).

[44] B. M. Weight, D. J. Weix, Z. J. Tonzetich, T. D. Krauss, and P. Huo, "Cavity quantum electrodynamics enables para- and ortho-selective electrophilic bromination of nitrobenzene," Journal of the American Chemical Society **0**, null (0), pMID: 38814893, https://doi.org/10.1021/jacs.4c04045.

[45] J. D. Weidman, M. S. Dadgar, Z. J. Stewart, B. G. Peyton, I. S. Ulusoy, and A. K. Wilson, "Cavity-modified molecular dipole switching dynamics," The Journal of Chemical Physics **160**, 094111 (2024), https://pubs.aip.org/aip/jcp/article-pdf/doi/10.1063/5.0188471/19708269/094111_1_5.0188471.pdf.

[46] B. G. Peyton, J. D. Weidman, and A. K. Wilson, "Light-induced electron dynamics of molecules in cavities: comparison of model hamiltonians," J. Opt. Soc. Am. B **41**, C74–C81 (2024).

[47] Y. E. Moutaoukal, R. R. Riso, M. Castagnola, and H. Koch, "Towards polaritonic molecular orbitals for large molecular systems," (2024), arXiv:2406.15052 [physics.chem-ph].

[48] M. Matoušek, N. Vu, N. Govind, J. J. F. IV, and L. Veis, "Polaritonic chemistry using the density matrix renormalization group method," (2024), arXiv:2407.01381 [physics.chem-ph].

[49] M. D. Liebenthal and A. E. D. III, "The orientation dependence of cavity-modified chemistry," (2024), arXiv:2405.01676 [physics.chem-ph].

[50] M. T. Lexander, S. Angelico, E. F. Kjønstad, and H. Koch, "Analytical evaluation of ground state gradients in quantum electrodynamics coupled cluster theory," (2024), arXiv:2406.08107 [physics.chem-ph].

[51] L. Monzel and S. Stopkowicz, "Diagrams and symmetry in polaritonic coupled cluster theory," (2024), arXiv:2407.00757 [physics.chem-ph].

[52] J. R. Schrieffer and P. A. Wolff, "Relation between the anderson and kondo hamiltonians," Phys. Rev. **149**, 491–492 (1966).

[53] F. J. Wegner, "Flow equations for hamiltonians," Nuclear Physics B - Proceedings Supplements **90**, 141–146 (2000), nON-PERTURBATIVE QCD AND HADRON PHENOMENOLOGY.

[54] T. Helgaker, P. Jorgensen, and J. Olsen, *Molecular electronic-structure theory* (John Wiley & Sons, 2014).

[55] F. A. Evangelista, "A driven similarity renormalization group approach to quantum many-body problems," The Journal of Chemical Physics **141**, 054109 (2014), https://pubs.aip.org/aip/jcp/article-pdf/doi/10.1063/1.4890660/13374939/054109_1_online.pdf.

[56] K. Kowalski and N. P. Bauman, "Fock-space schrieffer–wolff transformation: Classically-assisted rank-reduced quantum phase estimation algorithm," Applied Sciences **13**, 539 (2023).

[57] S. D. Folkestad, E. F. Kjønstad, R. H. Myhre, J. H. Andersen, A. Balbi, S. Coriani, T. Giovannini, L. Goletto, T. S. Haugland, A. Hutcheson, I.-M. Høyvik, T. Moitra, A. C. Paul, M. Scavino, A. S. Skeidsvoll, Å. H. Tveten, and H. Koch, "et 1.0: An open source electronic structure program with emphasis on coupled cluster and multilevel methods," J. Chem. Phys. **152**, 184103 (2020).

[58] A. Mandal, S. M. Vega, and P. Huo, "Polarized fock states and the dynamical casimir effect in molecular cavity quantum electrodynamics," J. Phys. Chem. Lett. **11**, 9215–9223 (2020).

[59] "Molecular orbital theory in cavity qed environments," Nat. Commun. **13**, 1368 (2022).

[60] X. Li and Y. Zhang, "First-principles molecular quantum electrodynamics theory at all coupling strengths," (2023), arXiv:2310.18228 [physics.chem-ph].

[61] F. J. J. Manderna R, Vu N, "Comparing parameterized and self-consistent approaches to ab initio cavity quantum electrodynamics for electronic strong coupling," (2024).

[62] H. Spohn, *Dynamics of charged particles and their radiation field* (Cambridge Univ. Press, Cambridge, 2004).

[63] A. Szabo and N. S. Ostlund, *Modern Quantum Chemistry: Introduction to Advanced Electronic Structure Theory*, 1st ed. (Dover Publications, Inc., Mineola, 1996).

[64] R. H. Myhre, T. J. A. Wolf, L. Cheng, S. Nandi, S. Coriani, M. Gühr, and H. Koch, "A theoretical and experimental benchmark study of core-excited states in nitrogen," J. Chem. Phys. **148**, 064106 (2018).

[65] N. M. Hoffmann, C. Schäfer, A. Rubio, A. Kelly, and H. Appel, "Capturing vacuum fluctuations and photon correlations in cavity quantum electrodynamics with multitrajectory ehrenfest dynamics," Phys. Rev. A **99**, 063819 (2019).

[66] N. Vu, J. J. F. IV, and R. Manderna, "Qed-ci: A program for performing cavity quantum electrodynamics configuration interaction calculations," (2023), https://github.com/mapol-chem/qed-ci/tree/main (last accessed July 2024).

[67] D. G. A. Smith, L. A. Burns, A. C. Simmonett, R. M. Parrish, M. C. Schieber, R. Galvelis, P. Kraus, H. Kruse, R. Di Remigio, A. Alenaizan, A. M. James, S. Lehtola, J. P. Misiewicz, M. Scheurer, R. A. Shaw, J. B. Schriber, Y. Xie, Z. L. Glick, D. A. Sirianni, J. S. O'Brien, J. M. Waldrop, A. Kumar, E. G. Hohenstein, B. P. Pritchard, B. R. Brooks, H. F. Schaefer, A. Y. Sokolov, K. Patkowski, A. E. DePrince, U. Bozkaya, R. A. King, F. A. Evangelista, J. M. Turney, T. D. Crawford, and C. D. Sherrill, "Psi4 1.4: Open-source software for high-throughput quantum chemistry," J. Chem. Phys. **152**, 184108 (2020).

[68] D. G. A. Smith, L. A. Burns, D. A. Sirianni, D. R. Nascimento, A. Kumar, A. M. James, J. B. Schriber, T. Zhang, B. Zhang, A. S. Abbott, E. J. Berquist, M. H. Lechner, L. A. Cunha, A. G. Heide, J. M. Waldrop, T. Y. Takeshita, A. Alenaizan, D. Neuhauser, R. A. King, A. C. Simmonett, J. M. Turney, H. F. Schaefer, F. A. Evangelista, A. E. D. III, T. D. Crawford, K. Patkowski, and C. D. Sherrill, "Psi4numpy: An interactive quantum chemistry programming environment for reference implementations and rapid development," J. Chem. Theory Comput. **14**, 3504–3511 (2018).

[69] J. Dunning, Thom H., "Gaussian basis sets for use in correlated molecular calculations. I. The atoms boron through neon and hydrogen," The Journal of Chemical Physics **90**, 1007–1023 (1989), https://pubs.aip.org/aip/jcp/article-pdf/90/2/1007/18974738/1007_1_online.pdf.

[70] R. Krishnan, J. S. Binkley, R. Seeger, and J. A. Pople, "Self-consistent molecular orbital methods. xx. a basis set for correlated wave functions," J. Chem. Phys. **72**, 650–654 (1980).